scientific reports

OPEN

Efficient oxidation of sulfides to sulfoxides catalyzed by heterogeneous Zr-containing polyoxometalate grafted on graphene oxide

Zahra Yekke-Ghasemi[1], Majid M. Heravi[1]✉, Masoume Malmir[1] & Masoud Mirzaei[2,3]✉

In this study, a tri-component composite named $Zr/SiW_{12}/GO$ was meticulously prepared through an ultrasonic-assisted method. This composite incorporates zirconium nanoparticles (Lewis acid), a negatively charged Keggin type polyoxometalate, and graphene oxide, and serves as a remarkable heterogeneous catalyst. The Keggin component plays multiple roles as reducing, encapsulating, and bridging agents, resulting in a cooperative effect among the three components that significantly enhances the catalytic activity. The catalytic performance of $Zr/SiW_{12}/GO$ was thoroughly investigated in the oxidation of sulfides to sulfoxides under mild conditions, employing H_2O_2 as the oxidant. Remarkably, this composite exhibited exceptional stability and could be effortlessly recovered and reused up to four times without any noticeable loss in its catalytic activity.

The incorporation of sulfoxide moiety is of great significance in the structure of biomolecules and synthetic intermediates, which are widely utilized in the production of various biological and chemical products[1,2]. The oxidation of sulfides to sulfoxides represents the simplest synthetic route for obtaining sulfoxides, and numerous oxidative reagents and methods have been developed for this conversion[3,4]. However, the pursuit of selective catalytic oxidation using environmentally friendly oxidants is a crucial and demanding objective for the chemical industry[5,6], with dilute hydrogen peroxide being one such oxidant[7]. The favorable properties of aqueous hydrogen peroxide have prompted the development of several valuable methods for the oxidation of sulfides to sulfoxides and sulfones, employing diverse catalysts. Recently, a wide range of catalysts containing transition metals incorporated within frameworks or grafted onto solid surfaces have been prepared and explored for various oxidations in the presence of H_2O_2[8–16]. Among these catalysts, those containing metal species[17–20], particularly zirconium, have demonstrated remarkable catalytic activity. Nevertheless, these systems have exhibited certain drawbacks, such as the requirement for the recovery of expensive catalysts, presence of residual metals in the final products, and formation of allylic oxidation products. Consequently, the development of a novel, environmentally friendly method that can overcome these challenges represents a highly challenging task.

Polyoxometalates (POMs) are a subset of metal-oxide clusters that exhibit a wide range of sizes, ranging from nanometers to several micrometers. Their diverse structures, sizes, photochemistry, redox chemistry, and charge distribution make them crucial in emerging fields such as sensors[21], catalysts[22–24], medicine[25], magnetism[26] and batteries[27]. The high stability of the redox states of POMs allows them to act as electron reservoirs, giving rise to mixed valence state species that are important in their use as catalysts[28]. Generally, POMs are formed from combinations of metal oxide building blocks with a general formula of [MOx]n (M is referred to as the addendum atom and is a transition metal), creating anionic clusters that can also contain cations (known as heteroatoms) such as B^{3+}, Si^{4+} and P^{5+} further diversifying and complicating their chemistry. Based on the presence or absence of heteroatoms, POMs can be categorized as heteropolyanions or isopolyanions.

Keggin-type polyoxoanions with the formula $[XM_{12}O_{40}]^{n-}$ (X represents the heteroatom, and M represents the addendum atom) benefit from a unique and highly symmetrical structure that exhibits exceptional stability

[1]Department of Organic Chemistry, Faculty of Chemistry, Alzahra University, Tehran, Iran. [2]Department of Chemistry, Faculty of Science, Ferdowsi University of Mashhad, Mashhad 9177948974, Iran. [3]Khorasan Science and Technology Park (KSTP), 12Th Km of Mashhad-Quchan Road, MashhadKhorasan Razavi 9185173911, Iran. ✉email: mmheravi@alzahra.ac.ir; mirzaeesh@um.ac.ir

under various conditions, making them a subject of extensive study. Furthermore, by altering the constituent metals, their thermal or chemical stability and acidity properties at the atomic/molecular level can be controlled without affecting the Keggin structure. Keggin-type polyoxoanions have been widely employed in several catalytic applications due to their significant characteristics. For example, their large negative charges enable them to act as Lewis bases, and when partially or fully protonated, they can facilitate acid-catalyzed reactions as Brönsted acids, such as esterification and hydrolysis. The presence of certain metal ions with unoccupied orbitals allows them to act as Lewis acids, and their ability to undergo reversible, multi-electron redox processes makes them suitable catalysts for the oxidation of alcohols, alkanes, and olefins[29]. It is important to note that Keggin-type POMs, like other members of their family, are generally soluble in aqueous solutions, making catalyst recovery challenging from these media. To overcome this issue, heterogeneous systems such as the formation of composites or hybrids of POMs using solid supports with high surface areas like carbon nanomaterials or MOFs have been actively explored[30–32]. The use of larger-sized cations or organic cations, such as dimethyldioctadecylammonium or tetrabutylammonium salts, for charge balance has also been investigated. Notably, Zr-containing POMs have exhibited pronounced catalytic activity in various reactions, including oxidation reactions, due to the presence of open coordination sites on the Zr center[13,33–35].

Composites comprising of POMs, metal nanoparticles (NPs), and carbon nanomaterials can be formed through covalent linkage, non-covalent interactions, or electrostatic attachment methods, such as layer by layer assembly. For instance, POMs can be incorporated into graphene (G) or graphene oxide (GO) networks using a green and straightforward wet-chemical synthesis approach, wherein the POMs undergo a redox reaction, transitioning from the reduced polyblue form to a neutral form, and acting as intermolecular linkers.

In our ongoing investigation of the preparation and application of heterogeneous catalysts[36–43], with a particular focus on POM-based catalysts[44–46], we present a tri-component composite heterogeneous **Zr/SiW$_{12}$/GO** catalyst for the oxidation of sulfides to sulfoxides using hydrogen peroxide. As anticipated, **Zr/SiW$_{12}$/GO** functions simultaneously as a Lewis acid/base, enhancing catalytic activity by combining the zirconium Lewis acid with the negatively charged Keggin species on the GO support (Fig. 1). Additionally, we have examined the recyclability of the **Zr/SiW$_{12}$/GO** catalyst to assess its nature and stability.

Result and discussion
### Synthesis and characterization of catalysts
The tricomponent **Zr/SiW$_{12}$/GO** composite was synthesized by a simple reaction in an ultrasonic bath (Fig. 1). During synthesis, the introduction of the GO support into the composite can effectively increase the specific surface area of the composite for the dispersion of Zr nanoparticles and SiW$_{12}$ species with the electrostatic interaction between negatively charged, reduced SiW$_{12}$ units preventing the Zr NPs from aggregating. This agrees with prior reports that smaller Zr NPs rather than POM units can be affixed to the walls of the GO by the selection of the proper concentration of the reduced SiW$_{12}$[47,48].

Scanning electron microscopy (SEM) and transmission electron microscopy (TEM) were employed to ascertain the structure and morphology of the GO and Zr/SiW$_{12}$/GO composite (Fig. 2a).

In situ energy dispersive X-ray analysis (Fig. 2c) showed strong tungsten and carbon peaks accompanied by Zr peaks, confirming the existence of all three components in this composite. The TEM observations are consistent with these results (Fig. 2b).
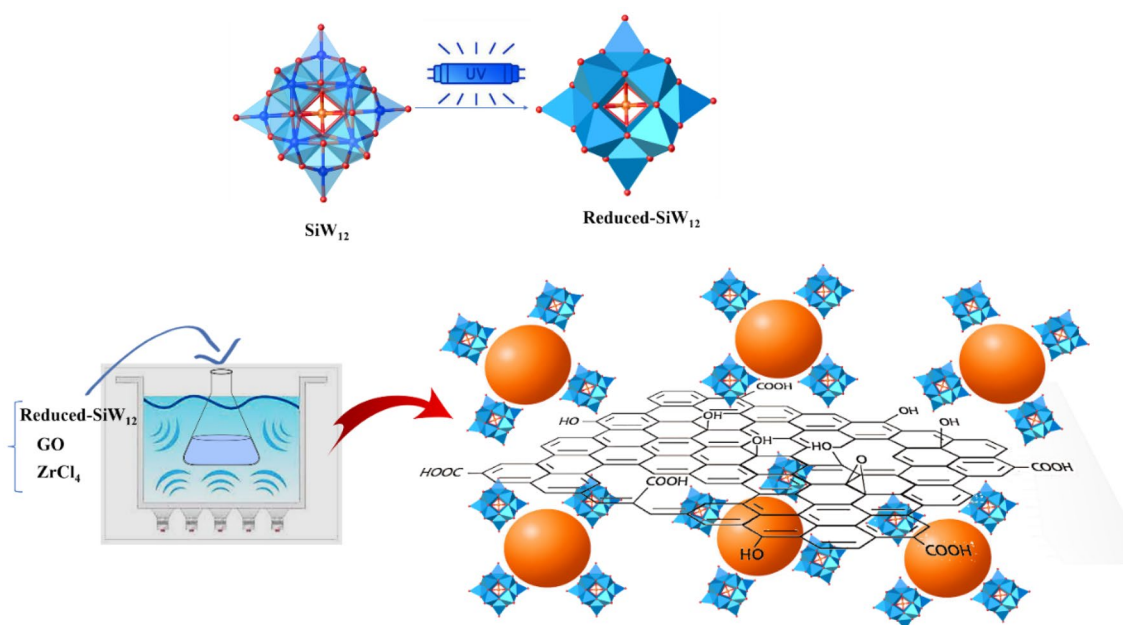

Figure 1. Synthetic route of **Zr/SiW$_{12}$/GO** tricomponent catalyst with representation of SiW$_{12}$ (polyhedral representation), Zr (orange ball representation), and GO.
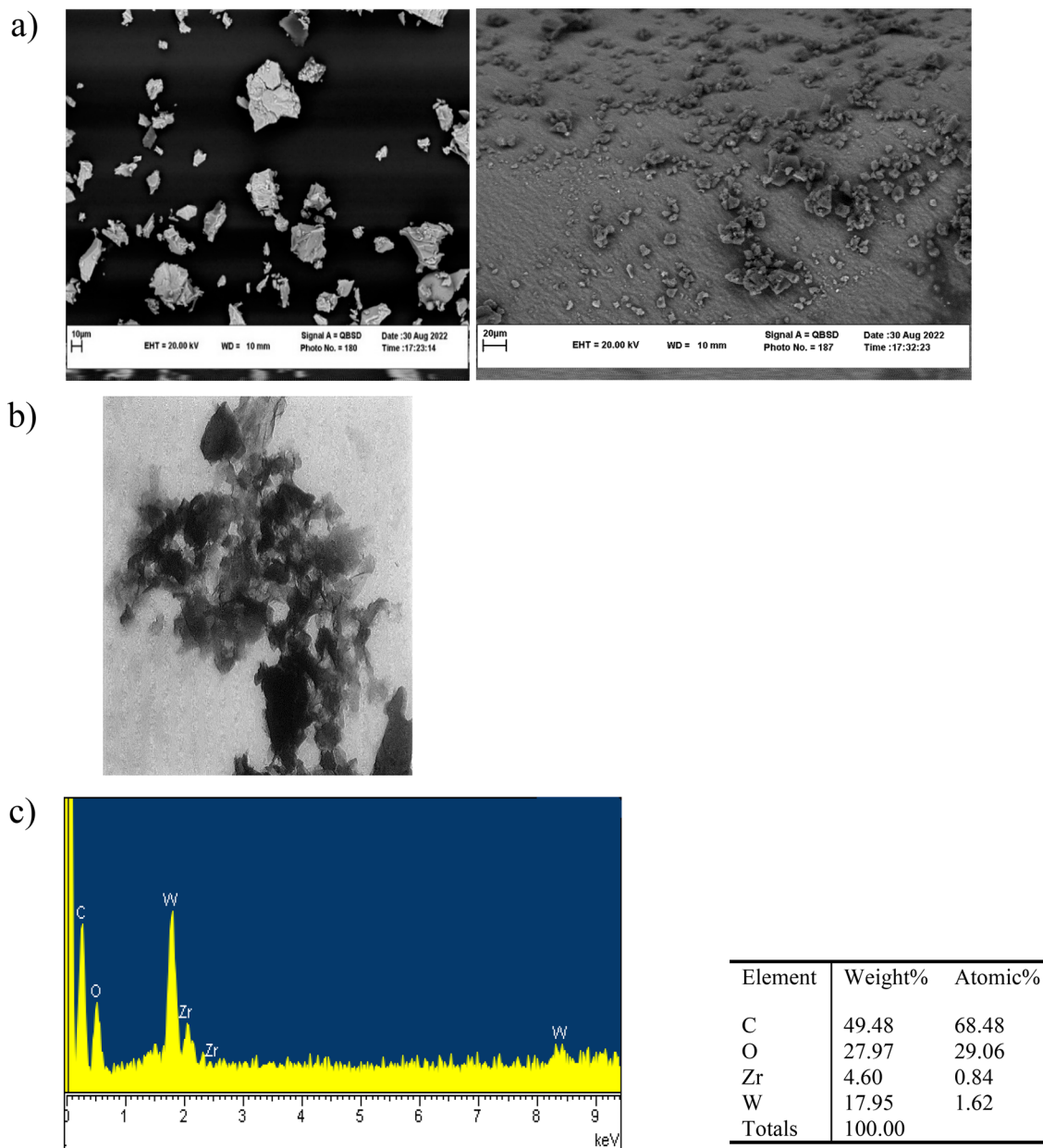
Figure 2. (**a**) SEM images of GO (right) and **Zr/SiW$_{12}$/GO** composite (left); (**b**) TEM image of **Zr/SiW$_{12}$/GO** composite; (**c**) EDX analysis of **Zr/SiW$_{12}$/GO**.

The powder XRD patterns of SiW$_{12}$, GO, and the **Zr/SiW$_{12}$/GO** composite are depicted in Fig. 3. The GO exhibits a distinct diffraction peak at 9.8°, corresponding to the interlayer spacing of C (002) at 0.790 nm. The absence of any peak at a 2θ value of 26.5° confirms the complete oxidation of G. Moreover, the **Zr/SiW$_{12}$/GO** composite displays diffraction peaks for both SiW$_{12}$ and GO (notably, the characteristic peaks at 9°–11° for 2θ value), providing evidence for the formation of a tricomponent composite.

Furthermore, FT-IR spectra were obtained to analyze the chemical structure of the **Zr/SiW$_{12}$/GO** composite. These spectra exhibit a vibration pattern akin to that of SiW$_{12}$ and GO individually, thereby confirming the presence of both constituents within the composite (as shown in Fig. 4). The characteristic bands in the range of $600-1100$ cm^{-1} can be attributed to the vibrations of SiW$_{12}$, with strong bands observed for W–O$_c$, W–O$_t$, W–O$_b$ and Si–O stretching vibrations at approximately 875, 801, 970, and 921 cm^{-1}, respectively. Additionally, the bands at 1221, 1436, 1520, and 1647 cm^{-1} correspond to the stretching vibration of C=C and C=O bonds in GO. Notably, the band associated with carboxylic acid groups in GO, originally observed at 1710 cm^{-1}, is shifted to 1627 cm^{-1} in the composite. This shift indicates the formation of robust hydrogen bonds between the oxygen atoms of SiW$_{12}$ and the hydroxyl groups on the carboxylic acids.
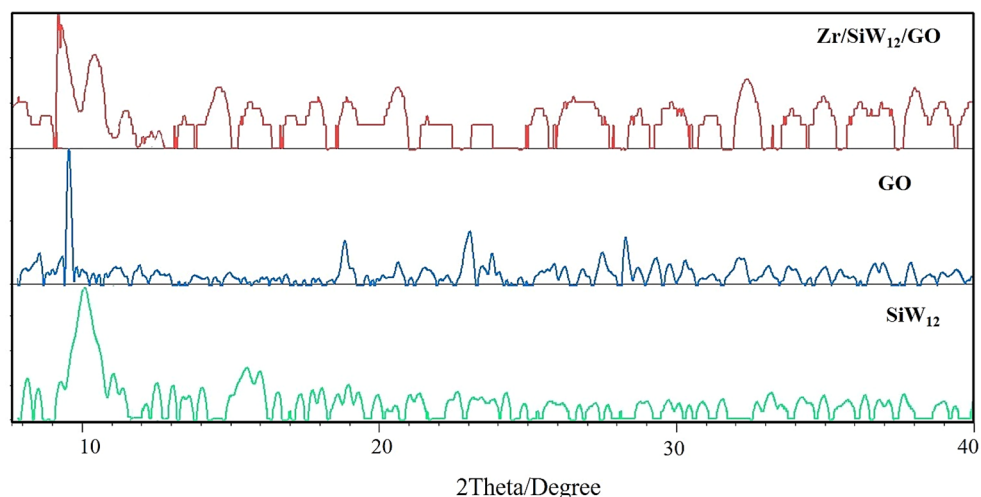
Figure 3. XRD patterns of the **Zr/SiW$_{12}$/GO** composite, GO and SiW$_{12}$.
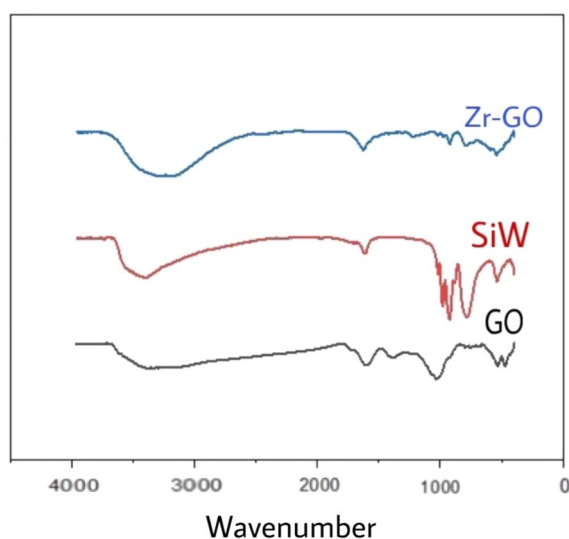
Figure 4. FTIR spectra of SiW$_{12}$, GO and the **Zr/SiW$_{12}$/GO** composite.

Catalytic activity

The catalytic activity of the **Zr/SiW$_{12}$/GO** composite was investigated for the oxidation of methylphenyl sulfide (MPS) to methylphenyl sulfoxide using aqueous hydrogen peroxide (30%) under solvent-free conditions at room temperature. In the absence of a catalyst, the reaction yielded only 45% of the desired product after 12 h (Table S1, entry 1). To enhance the reaction efficiency, MPS (1 mmol) was oxidized using **Zr/SiW$_{12}$/GO** (10 mg) and H_2O_2 (2 eq.) at room temperature, resulting in the formation of 95% sulfoxide in a significantly shorter reaction time (Table S1, entry 3).

Further investigations were conducted to determine the active site responsible for the oxidation of MPS in **Zr/SiW$_{12}$/GO**. Various catalysts including Zr-free POM[44,45] and Zr salts were examined. The results indicate that the presence of Zr is necessary for the oxidation of MPS, as confirmed by running the reaction in the presence of bare GO. Notably, Zr has been reported as one of the most effective metals for promoting the oxidation of sulfides[9]. While Zr salts exhibit reasonable catalytic activity, their separation and recovery from the reaction mixture pose challenges. In contrast, **Zr/SiW$_{12}$/GO** can be easily separated by filtration due to the presence of the GO support. Moreover, it demonstrated excellent reusability for up to four runs with consistently high yields. These findings suggest that the use of a substrate for heterogenization not only facilitates the separation process but also enhances the performance of the Zr active site, potentially attributed to the synergistic effect between GO, POM, and Zr.

To optimize the reaction conditions, various catalyst and oxidant loadings were investigated for the oxidation of MPS under S.F. and r.t. conditions (Table S1). Among the catalyst loadings tested (Table S1, entry 2–4), the use of 10 mg of **Zr/SiW$_{12}$/GO** yielded the highest product yield (Table S1, entry 3), while higher and lower catalyst

4

loadings resulted in lower yields. It is worth noting that sulfone is one of the main products in this reaction, as the oxidation of sulfides can be further converted into sulfone under continued oxidation conditions. However, when four equivalents of H_2O_2 were used, both products were obtained in impure form with different ratios, indicating that excessive oxidant leads to the production of side products and the progression of the oxidation process. Therefore, based on the results in Table S1, it was determined that 2.0 equivalents of H_2O_2 is the optimal amount. Additionally, MPS was oxidized with H_2O_2 using **Zr/SiW$_{12}$/GO** in various solvents (2.5 mL), and it was observed that not using any additional solvent resulted in better yields.

The effectiveness of the **Zr/SiW$_{12}$/GO** catalyst was further demonstrated by investigating the oxidation of different sulfides under the optimized conditions, revealing its efficacy for both aromatic and aliphatic sulfides (Table 1).

To gain insight into the mechanism, MPS oxidation over **Zr/SiW$_{12}$/GO** and H_2O_2 without any additional solvents was examined. Similar mechanisms have been reported in recent literature for this reaction[12,49,50]. Figure 5 presents a possible mechanism for the catalytic oxidation of sulfide over the **Zr/SiW$_{12}$/GO** composite. Initially, H_2O_2 can bind to **Zr/SiW$_{12}$/GO**, forming an active electrophilic peroxide intermediate. Subsequently, this peroxide- **Zr/SiW$_{12}$/GO** intermediate can undergo a nucleophilic attack by the -S atom of the sulfide, leading to the reduction of **Zr/SiW$_{12}$/GO** back to its original state for subsequent runs, with the release of one mole of water. Notably, the presence of Zr is crucial in facilitating the formation of the peroxide-metal complex and activating H_2O_2 molecules[51–53].

In the present study, the catalytic performance of the **Zr/SiW$_{12}$/GO** composite was compared with other recent reports on the oxidation of sulfides to sulfoxides (Table 2, entries 1–6). The results demonstrated that the **Zr/SiW$_{12}$/GO** composite exhibited superior performance in terms of reaction conditions and reaction times. Notably, this system offered the advantage of easy separation and high recyclability. The unique structure of SiW$_{12}$, which was well-stabilized on the surface of GO, contributed to the formation of a heterogeneous structure, as confirmed by the hot filtration test results.

Reusability of the catalyst

I agreement with the recent report[54], the recyclability of the **Zr/SiW$_{12}$/GO** catalyst was investigated using the model reaction under optimal conditions. After completion of the reaction, the mixture was triturated with Et_2O until it became clear, and the **Zr/SiW$_{12}$/GO** catalyst was separated by filtration. Subsequently, the catalyst was dried in air and examined again in the model reaction. As shown in Fig. S1, the **Zr/SiW$_{12}$/GO** catalyst could be successfully reused up to four times without significant loss of activity. However, when attempting to reuse the catalyst for the fifth reaction run, a dramatic decrease in catalytic performance was observed, resulting in a yield of only 65% for the model product. This decrease in activity can be attributed to the deposition of organic species on the catalyst during multiple reaction runs or the potential leaching of POM induced by $NaBH_4$, which may disrupt the catalyst structure and subsequently reduce its catalytic activity. To investigate this observation further, the leaching of Zr was examined after four and five reaction runs. It was found that upon reusing the catalyst for four reaction runs, there was a remarkable increase in Zr leaching, providing an explanation for the observed lower catalytic activity.

Subsequently, a standard hot filtration experiment[55] was conducted to ascertain the catalyst's composition for the synthesis of MPS under the optimal reaction conditions. The **Zr/SiW$_{12}$/GO** catalyst was extracted after achieving 40% conversion (t = 10 min), allowing the reactants to continue reacting. The results revealed that, subsequent to the catalyst's removal, there was minimal leaching of Zr, and the conversion rate reached 45% even

Entry	R^1	R^2	Time (min)	Yield (%)^a
1	C_6H_5	Me	20	95
2	C_6H_5	Et	35	94
3	C_6H_5	C_6H_5	60	83
4	p-MeC$_6$H$_4$	Me	63	80
5	p-BrC$_6$H$_4$	Me	50	90
6	p-O$_2$NC$_6$H$_4$	Me	40	87
7	p-HOC$_6$H$_4$	Me	30	90
8	Me	Me	60	90
9	Me	Et	70	77
10	CH_3	H	65	82

Table 1. Synthesis of sulfoxides by oxidation of sulfides over **Zr/SiW$_{12}$/GO** using H_2O_2 under S.F. and r.t. conditions. Reaction condition: a mixture of sulfide (1 mmol), H_2O_2 (2 eq.) with 4 drops EtOH and Zr/SiW$_{12}$/GO (10 mg) was stirred without any solvent. ^{a}Isolated yields.
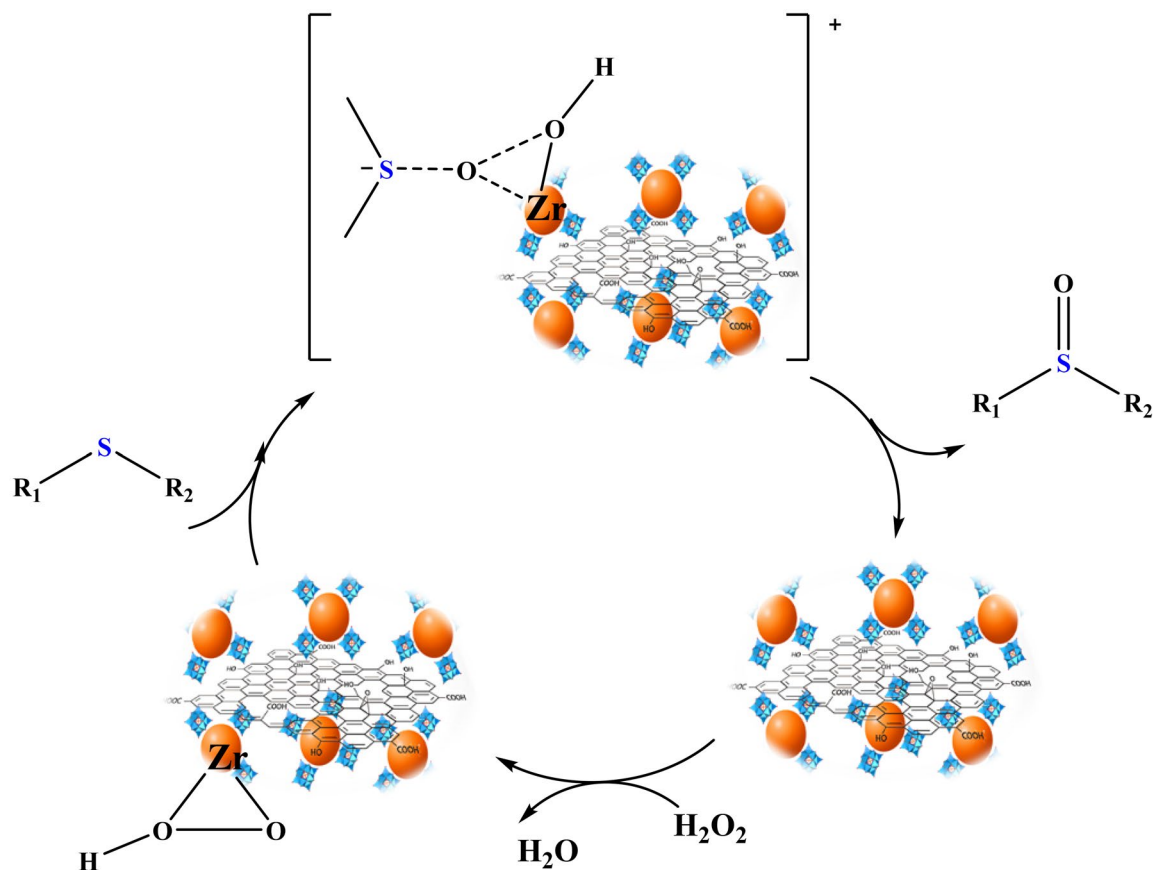
Figure 5. Schematic possible mechanism for the oxidation of sulfide catalyzed by **Zr/SiW$_{12}$/GO** and H$_2$O$_2$.

Entry	Catalyst (amount)	Conditions			Time (min)	Conversion (%)	Refs
		Oxidant	Solvent	Temp. or UV			
1	Mo$_6$W$_6$@EDMG (7 mg)	H$_2$O$_2$ (1.5 mmol)	EtOH	400 W lamp	120	88	[57]
2	MNP@TA-IL/W (0.4 mol%)	H$_2$O$_2$ (1.5 e.q)	H$_2$O	rt	60	98	[58]
3	Fe$_3$O$_4$@S-ABENZ@VO (5 mg)	H$_2$O$_2$ (16 mmol)	S.F	rt	80	98	[59]
4	VO(BINE)@Fe$_3$O$_4$ (30 mg)	H$_2$O$_2$ (2 mmol)	S.F	rt	5	96	[14]
5	PAMAM-G1-PMo (50 mg)	H$_2$O$_2$ (0.55 mmol)	MeOH	rt	240	88	[60]
6	Zr/SiW$_{12}$/GO (10 mg)	H$_2$O$_2$ (2 mmol)	S.F	rt	30	98	This work

Table 2. Comparison of catalytic activity of **Zr/SiW$_{12}$/GO** with other reported catalysts for the oxidation of MPS.

after 40 min. Furthermore, analysis using ICP-OES demonstrated a Zr content of 0.002 mmol g^{-1} in the filtrate, which is negligible when compared to the initial loading of 0.27 mmol g^{-1}. These findings provided additional confirmation of the heterogeneous nature of the **Zr/SiW$_{12}$/GO** catalyst (Fig. 6).

Materials and methods
Chemicals
All chemicals were purchased from Merck (www.merckmillipore.com) and Sigma-Aldrich (www.sigmaaldrich.com) and used as received. Oxidation were conducted using sulfides, H$_2$O$_2$, acetonitrile, methanol, ethanol, and deionized water.

Instrumentation
The infrared spectra of the catalysts were recorded on a Thermo Nicolet/AVATAR 370 Fourier transform spectrophotometer. The morphology of the catalyst was studied by scanning electron microscopy (SEM) using a Leo 1450 VP, Germany instrument. Powder XRD patterns were obtained using a PANalytical B.V. diffractometer with Cu Kα radiation (λ = 1.54184 Å) at room temperature with a scan range 2θ = 5° to 50°, a step size of 0.05 °C
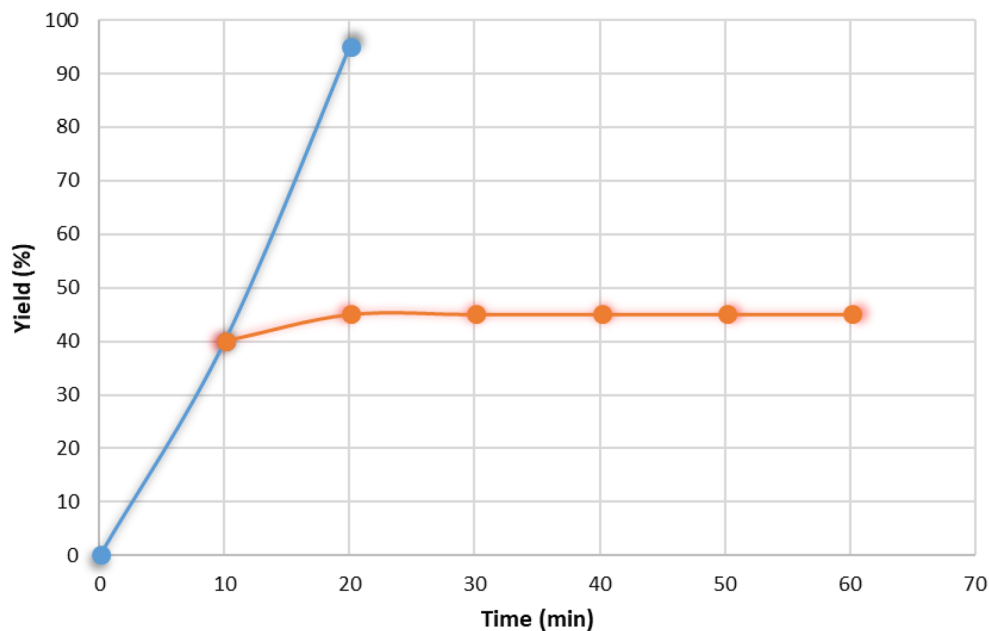
Figure 6. Monitoring of hot filtration experiment for the synthesis of MPS (blue line: with catalyst and red line: without catalyst).

and a step time of 1 s. The energy-dispersive X-ray (EDX) with resolution of about 500 nm (at an acceleration voltage of 10.00 kV and) was performed on a LEO-1450 VP unit (Zeiss, Germany).

Preparation of catalyst

Graphene oxide (GO) was synthesized according to Kigozi, M. (2020) method and characterized by Powder XRD, SE M and FT-IR,[56]. The tricomponent catalyst was prepared with GO, reduced $H_4SiW_{12}O_{40}$ (SiW_{12}), and $ZrCl_4$.

Synthesis of $Zr/SiW_{12}/GO$ composite

An aqueous solution of SiW_{12} (0.5 mmol, 10 mL) was adjusted to the pH 1.18 and 1 mL of isopropanol was added. The solution was reduced photochemically with a UV light source (500 W Hg lamp) until the color of the solution become blue–black (approximate time = 30 min). The solution of reduced SiW_{12} added to GO (10 mL, and 8 mg mL^{-1}) and $ZrCl_4$ (0.5 mM) at room temperature in an ultrasonic bath. After 120 min of reaction, the tricomponent composites were assembled. The samples were centrifuged and then washed with H_2O.

Yield: 0.26 g (13% based on W). FT-IR (KBr pellet, cm^{-1}): 3272, 3184, 1627, 1510, 1231, 1081, 971, 924, 794, 746, 591, 544.

Typical method for the catalytic oxidation of sulfides to sulfoxides

A 50 mL round bottom flask was charged with 1 mmol of sulfide, 10 mg of the **$Zr/SiW_{12}/GO$** catalyst, and four drops of 96% EtOH. The resulting solution was stirred at room temperature, and 0.227 g (2 eq.) of 30 wt% H_2O_2 was slowly added. The reaction progress was monitored by TLC using a mixture of n-hexane and EtOAc (8:2) as the solvent system. Once the oxidation was complete, the **$Zr/SiW_{12}/GO$** catalyst was filtered off and separated from the mixture by filtration. It was then washed with 95% EtOH and dried in a vacuum at room temperature overnight for recycling purposes. The reaction filtrate was washed with diethyl ether (3 × 7 mL), and the combined organic layers were dehydrated using Na_2SO_4. The crude products were purified by column chromatography on a silica gel column using n-hexane/ethyl acetate (8:2) as the eluent, resulting in the desired products. The ^{1}HNMR spectrum for the corresponding methyl phenyl sulfoxide can be found online in the Supplementary Information (Fig. S2).

Conclusion

In conclusion, we have successfully developed a sonochemical method for preparing a tri-component composite catalyst, **$Zr/SiW_{12}/GO$**, for the catalytic oxidation of sulfides. This catalyst offers several advantages over previous solid supports, including high activity, stability, and improved recoverability. The incorporation of GO in the Zr-containing POMs provides enhanced recycling capability by stabilizing the active site dispersion. The combination of GO and Zr-containing POMs allows for effective oxidation and easy separation of the supported-catalyst active sites in the reaction system. The **$Zr/SiW_{12}/GO$** catalyst can be easily recycled through filtration and reused up to four times without significant loss of activity.

Data availability

All data generated or analysed during this study are included in this published article [and its supplementary information files].

References

1. Sipos, G., Drinkel, E. E. & Dorta, R. The emergence of sulfoxides as efficient ligands in transition metal catalysis. *Chem. Soc. Rev.* **44**, 3834–3860 (2015).
2. Yan, Q. *et al.* Highly efficient enantioselective synthesis of chiral sulfones by Rh-catalyzed asymmetric hydrogenation. *J. Am. Chem. Soc.* **141**, 1749–1756 (2019).
3. Chakravarthy, R. D., Ramkumar, V. & Chand, D. K. A molybdenum based metallomicellar catalyst for controlled and selective sulfoxidation reactions in aqueous medium. *Green Chem.* **16**, 2190 (2014).
4. Yang, C. *et al.* Tetra-(tetraalkylammonium)octamolybdate catalysts for selective oxidation of sulfides to sulfoxides with hydrogen peroxide. *Green Chem.* **11**, 1401 (2009).
5. Cavani, F. & Teles, J. H. Sustainability in catalytic oxidation: An Alternative Approach Or A Structural Evolution?. *ChemSusChem* **2**, 508–534 (2009).
6. Mizuno, N. *Modern Heterogeneous Oxidation Catalysis* (WILEY-VCH Verlag GmbH & Co. KGaA, 2009).
7. Campos-Martin, J. M., Blanco-Brieva, G. & Fierro, J. L. G. Hydrogen peroxide synthesis: An outlook beyond the anthraquinone process. *Angew. Chem. Int. Ed.* **45**, 6962–6984 (2006).
8. Faccioli, F. *et al.* Hydrolytic stability and hydrogen peroxide activation of zirconium-based oxoclusters. *Eur. J. Inorg. Chem.* **2015**, 210–225 (2015).
9. Hajjami, M., Shiri, L. & Jahanbakhshi, A. Zirconium oxide complex-functionalized MCM-41 nanostructure: An efficient and reusable mesoporous catalyst for oxidation of sulfides and oxidative coupling of thiols using hydrogen peroxide. *Appl. Organomet. Chem.* **29**, 668–673 (2015).
10. Tamoradi, T., Ghorbani-Choghamarani, A. & Ghadermazi, M. Synthesis of new zirconium complex supported on MCM-41 and its application as an efficient catalyst for synthesis of sulfides and the oxidation of sulfur containing compounds. *Appl. Organomet. Chem.* **32**, e4340 (2018).
11. Wang, J. *et al.* Zr(IV)-based metal-organic framework nanocomposites with enhanced peroxidase-like activity as a colorimetric sensing platform for sensitive detection of hydrogen peroxide and phenol. *Environ. Res.* **203**, 111818 (2022).
12. Zhang, P.-Y., Wang, Y., Yao, L.-Y. & Yang, G.-Y. Hepta-Zr-incorporated polyoxometalate assembly. *Inorg. Chem.* **61**, 10410–10416 (2022).
13. Maksimchuk, N. V. *et al.* Activation of H2O2 over Zr(IV). Insights from model studies on Zr-monosubstituted lindqvist tungstates. *ACS Catal.* **11**, 10589–10603 (2021).
14. Veisi, H., Rashtiani, A., Rostami, A., Shirinbayan, M. & Hemmati, S. Chemo-selective oxidation of sulfide to sulfoxides with H_2O_2 catalyzed by oxo-vanadium/Schiff-base complex immobilized on modified magnetic Fe_3O_4 nanoparticles as a heterogeneous and recyclable nanocatalyst. *Polyhedron* **157**, 358–366 (2019).
15. Ivanchikova, I. D., Maksimchuk, N. V., Skobelev, I. Y., Kaichev, V. V. & Kholdeeva, O. A. Mesoporous niobium-silicates prepared by evaporation-induced self-assembly as catalysts for selective oxidations with aqueous H_2O_2. *J. Catal.* **332**, 138–148 (2015).
16. Thornburg, N. E., Thompson, A. B. & Notestein, J. M. Periodic trends in highly dispersed groups IV and V supported metal oxide catalysts for alkene epoxidation with H_2O_2. *ACS Catal.* **5**, 5077–5088 (2015).
17. Mary Imelda Jayaseeli, A., Ramdass, A. & Rajagopal, S. Selective H_2O_2 oxidation of organic sulfides to sulfoxides catalyzed by cobalt(III)–salen ion. *Polyhedron* **100**, 59–66 (2015).
18. Jiang, J., Luo, R., Zhou, X., Chen, Y. & Ji, H. Photocatalytic properties and mechanistic insights into visible light-promoted aerobic oxidation of sulfides to sulfoxides via tin porphyrin-based porous aromatic frameworks. *Adv. Synth. Catal.* **360**, 4402–4411 (2018).
19. Heidari, L. & Shiri, L. CoFe$_2$O$_4$@SiO$_2$-CPTES-Guanidine-Cu(II): A novel and reusable nanocatalyst for the synthesis of 2,3-dihydroquinazolin-4(1H)-ones and polyhydroquinolines and oxidation of sulfides. *Appl. Organomet. Chem.* **33**, e4636 (2019).
20. Han, M. *et al.* A crown-shaped Ru-substituted arsenotungstate for selective oxidation of sulfides with hydrogen peroxide. *Chemistry* **24**, 11059–11066 (2018).
21. Zhou, C., Li, S., Zhu, W., Pang, H. & Ma, H. A sensor of a polyoxometalate and Au-Pd alloy for simultaneously detection of dopamine and ascorbic acid. *Electrochim. Acta* **113**, 454–463 (2013).
22. Narkhede, N., Singh, S. & Patel, A. Recent progress on supported polyoxometalates for biodiesel synthesis via esterification and transesterification. *Green Chem.* **17**, 89–107 (2015).
23. Lotfian, N., Heravi, M. M., Mirzaei, M. & Daraie, M. Investigation of the uncommon basic properties of [Ln(W$_5$O$_{18}$)$_2$]$^{9-}$ (Ln = La, Ce, Nd, Gd, Tb) by changing central lanthanoids in the syntheses of pyrazolopyranopyrimidines. *J. Mol. Struct.* **1199**, 126953 (2020).
24. Heravi, M. M. *et al.* H$_5$BW$_{12}$O$_{40}$ as a green and efficient homogeneous but recyclable catalyst in the synthesis of 4H-Pyrans via multicomponent reaction. *Appl. Organomet. Chem.* **32**, e4479 (2018).
25. Arefian, M., Mirzaei, M., Eshtiagh-Hosseini, H. & Frontera, A. A survey of the different roles of polyoxometalates in their interaction with amino acids, peptides and proteins. *Dalton Trans.* **46**, 6812–6829 (2017).
26. Khoshkhan, Z. *et al.* Two polyoxometalate-based hybrids constructed from trinuclear lanthanoid clusters with single-molecule magnet behavior. *Polyhedron* **194**, 114903 (2021).
27. Wang, H. *et al.* In Operando X-ray absorption fine structure studies of polyoxometalate molecular cluster batteries: Polyoxometalates as electron sponges. *J. Am. Chem. Soc.* **134**, 4918–4924 (2012).
28. Li, N., Liu, J., Dong, B. & Lan, Y. Polyoxometalate-based compounds for photo- and electrocatalytic applications. *Angew. Chem. Int. Ed.* **59**, 20779–20793 (2020).
29. Streb, C. New trends in polyoxometalate photoredox chemistry: From photosensitisation to water oxidation catalysis. *Dalton Trans.* **41**, 1651–1659 (2012).
30. Derakhshanrad, S., Mirzaei, M., Streb, C., Amiri, A. & Ritchie, C. Polyoxometalate-based frameworks as adsorbents for drug of abuse extraction from hair samples. *Inorg. Chem.* **60**, 1472–1479 (2021).
31. Akbari, M., Mirzaei, M. & Amiri, A. Synergistic effect of lacunary polyoxotungstates and carbon nanotubes for extraction of organophosphorus pesticides. *Microchem. J.* **170**, 106665 (2021).
32. Amiri, A., Mirzaei, M. & Derakhshanrad, S. A nanohybrid composed of polyoxotungstate and graphene oxide for dispersive micro solid-phase extraction of non-steroidal anti-inflammatory drugs prior to their quantitation by HPLC. *Microchim. Acta* **186**, 534 (2019).
33. Kholdeeva, O. A. *et al.* Zr IV—monosubstituted keggin-type dimeric polyoxometalates: Synthesis, characterization, catalysis of H$_2$O$_2$-based oxidations, and theoretical study. *Inorg. Chem.* **45**, 7224–7234 (2006).

34. Aoto, H. *et al.* Zirconium(IV)- and hafnium(IV)-containing polyoxometalates as oxidation precatalysts: Homogeneous catalytic epoxidation of cyclooctene by hydrogen peroxide. *J. Mol. Catal. A Chem.* **394**, 224–231 (2014).
35. Li, D. *et al.* Modification of tetranuclear zirconium-substituted polyoxometalates—syntheses, structures, and peroxidase-like catalytic activities. *Eur. J. Inorg. Chem.* **2013**, 1926–1934 (2013).
36. Sadjadi, S., Lazzara, G., Malmir, M. & Heravi, M. M. Pd nanoparticles immobilized on the poly-dopamine decorated halloysite nanotubes hybridized with N-doped porous carbon monolayer: A versatile catalyst for promoting Pd catalyzed reactions. *J. Catal.* **366**, 245–257 (2018).
37. Sadjadi, S., Malmir, M., Lazzara, G., Cavallaro, G. & Heravi, M. M. Preparation of palladated porous nitrogen-doped carbon using halloysite as porogen: Disclosing its utility as a hydrogenation catalyst. *Sci. Rep.* **10**, 2039 (2020).
38. Heravi, M. M. & Mohammadkhani, L. *Synthesis of Various N-Heterocycles Using the Four-Component Ugi Reaction* 351–403 (2020). https://04.org/10.1016/bs.aihch.2019.04.001.
39. Heravi, M. M. & Talaei, B. *Ketenes as Privileged Synthons in the Synthesis of Heterocyclic Compounds Part 3* 195–291 (Elsevier, 2016). https://doi.org/10.1016/bs.aihch.2015.10.007.
40. Heravi, M. M. & Talaei, B. *Diketene as Privileged Synthon in the Syntheses of Heterocycles Part 1* 43–114 (Elsevier, 2017). https://doi.org/10.1016/bs.aihch.2016.10.003.
41. Amiri, Z., Malmir, M., Hosseinnejad, T., Kafshdarzadeh, K. & Heravi, M. M. Combined experimental and computational study on Ag-NPs immobilized on rod-like hydroxyapatite for promoting Hantzsch reaction. *Mol. Catal.* **524**, 112319 (2022).
42. Malmir, M., Heravi, M. M., Amiri, Z. & Kafshdarzadeh, K. Magnetic composite of γ-Fe$_2$O$_3$ hollow sphere and palladium doped nitrogen-rich mesoporous carbon as a recoverable catalyst for C-C coupling reactions. *Sci. Rep.* **11**, 22409 (2021).
43. Bisafar, M. B., Malmir, M. & Heravi, M. M. Highly selective reduction of nitro compounds catalyzed by MOF-derived glucose stabilized Fe$_3$O$_4$ under mild conditions. *J. Chem. Technol. Biotechnol.* https://doi.org/10.1002/jctb.7500 (2023).
44. Malmir, M., Heravi, M. M., Yekke-Ghasemi, Z. & Mirzaei, M. Incorporating heterogeneous lacunary Keggin anions as efficient catalysts for solvent-free cyanosilylation of aldehydes and ketones. *Sci. Rep.* **12**, 11573 (2022).
45. Yekke-Ghasemi, Z. *et al.* Fabrication of heterogeneous-based lacunary polyoxometalates as efficient catalysts for the multicomponent and clean synthesis of pyrazolopyranopyrimidines. *Inorg. Chem. Commun.* **140**, 109456 (2022).
46. Yekke-Ghasemi, Z., Heravi, M. M., Malmir, M. & Mirzaei, M. Monosubstituted Keggin as heterogeneous catalysts for solvent-free cyanosilylation of aldehydes and ketones. *Catal. Commun.* **171**, 106499 (2022).
47. Li, S. *et al.* Green chemical decoration of multiwalled carbon nanotubes with polyoxometalate-encapsulated gold nanoparticles: Visible light photocatalytic activities. *J. Mater. Chem.* **21**, 2282–2287 (2011).
48. Liu, R. *et al.* Facile synthesis of au-nanoparticle/polyoxometalate/graphene tricomponent nanohybrids: An enzyme-free electrochemical biosensor for hydrogen peroxide. *Small* **8**, 1398–1406 (2012).
49. Dang, T.-Y. *et al.* Tandem-like vanadium cluster chains in a polyoxovanadate-based metal–organic framework for efficient catalytic oxidation of sulfides. *Inorg. Chem. Front.* **8**, 4367–4375 (2021).
50. Li, H., Lian, C., Chen, L., Zhao, J. & Yang, G.-Y. Two unusual nanosized Nd 3+ -substituted selenotungstate aggregates simultaneously comprising lacunary Keggin and Dawson polyoxotungstate segments. *Nanoscale* **12**, 16091–16101 (2020).
51. Ghorbani-Choghamarani, A., Azadi, G., Tahmasbi, B., Hadizadeh-Hafshejani, M. & Abdi, Z. Practical and versatile oxidation of sulfides into sulfoxides and oxidative coupling of thiols using polyvinylpolypyrrolidonium tribromide. *Phosphorus. Sulfur. Silicon Relat. Elem.* **189**, 433–439 (2014).
52. Maciuca, A.-L., Ciocan, C.-E., Dumitriu, E., Fajula, F. & Hulea, V. V-, Mo- and W-containing layered double hydroxides as effective catalysts for mild oxidation of thioethers and thiophenes with H$_2$O$_2$. *Catal. Today* **138**, 33–37 (2008).
53. Li, B. *et al.* Iron-catalyzed selective oxidation of sulfides to sulfoxides with the polyethylene glycol/O$_2$ system. *Green Chem.* **14**, 130–135 (2012).
54. Sussanah, L. A matter of life(time) and death. *ACS Catal.* **8**, 8597–8599 (2018).
55. Sheldon, R. A., Wallau, M., Arends, I. W. C. E. & Schuchardt, U. Heterogeneous catalysts for liquid-phase oxidations: Philosophers' stones or trojan horses?. *Acc. Chem. Res.* **31**, 485–493 (1998).
56. Kigozi, M. *et al.* Synthesis and characterization of graphene oxide from locally mined graphite flakes and its supercapacitor applications. *Results Mater.* **7**, 100113 (2020).
57. Fakhri, H., Mahjoub, A., Nejat, R. & Maridiroosi, A. Fabrication of molybdenum-substituted tungstophosphoric acid immobilized onto functionalized graphene oxide: Visible light-induced photocatalyst for selective oxidation of sulfides to sulfoxides. *Inorg. Chem. Commun.* **123**, 108353 (2021).
58. Hosseini, S. H., Tavakolizadeh, M., Zohreh, N. & Soleyman, R. Green route for selective gram-scale oxidation of sulfides using tungstate/triazine-based ionic liquid immobilized on magnetic nanoparticles as a phase-transfer heterogeneous catalyst. *Appl. Organomet. Chem.* **32**, e3953 (2018).
59. Rezaei, S., Ghorbani-Choghamarani, A., Badri, R. & Nikseresht, A. Fe$_3$O$_4$@S-ABENZ@VO: Magnetically separable nanocatalyst for the efficient, selective and mild oxidation of sulfides and oxidative coupling of thiols. *Appl. Organomet. Chem.* **32**, e3948 (2018).
60. Tong, Q.-L. *et al.* The selective oxidation of sulfides to sulfoxides or sulfones with hydrogen peroxide catalyzed by a dendritic phosphomolybdate hybrid. *Catalysts* **9**, 791 (2019).

Acknowledgements

Author contributions

Z.Y.-G.: Methodology, Investigation, Formal analysis, Software, Writing-original draft preparation. M.M.H.: Main idea, Supervision, Funding acquisition, Conceptualization, Writing-review and editing, Visualization. M.Malmir: Methodology, Investigation, Formal analysis, Software, Writing-original draft preparation. M.Mirzaei: Main idea, Supervision, Funding acquisition, Conceptualization, Writing-review and editing, Visualization.

Competing interests

The authors declare no competing interests.

Additional information

Supplementary Information The online version contains supplementary material available at https://doi.org/10.1038/s41598-023-43985-z.

Correspondence and requests for materials should be addressed to M.M.H. or M.M.